

Applying the finite element method to analyze predischage lightning rods

Chin-Tsung HSIEH¹, Meng-Hui WANG^{1,*}, Cho-Yu PAN²

¹*Department of Electrical Engineering National Chin-Yi University of Technology,
Taichung, Taiwan, R. O. C.
e-mail: wangmh@ncut.edu.tw*

²*35 Lane 215 Chung-Shan Rd. Sec. 1, Taiping City, Taichung County 411 Taiwan, R. O. C.
e-mail: fred@ncut.edu.tw*

Received: 05.11.2009

Abstract

In this paper, the finite element method is applied for analyzing 4 types of lightning rods in order to select the optimal lightning rod configuration. First, software is used to calculate the 2D protective coverage of different lightning rods, and 4 kinds of typical lightning rods are simulated in different conditions. The analyzed results are then applied for the selection of the optimal lightning rod and the frame of the lightning rod. The analyzed results would be useful for electrical engineers to design lightning rods that offer the most effective lightning protection; the simulated results are also useful for the optimal location selection of lightning rods.

Key Words: *Finite element method, air terminal, discharge lightning rod*

1. Introduction

Due to rapid economic growth, buildings nowadays are built much higher than before. However, the higher the buildings, the more chances they have of being struck by lightning. Another factor causing lightning strikes to happening much more frequently in Taiwan might be the increasing numbers of electric towers and transformer stations built to meet the fast-growing electricity demands from technology industries [1-2]. With more large buildings and power plants exposed to the atmosphere, lightning strikes would happen much more regularly than before and cause more severe fires, injuries, deaths, or enormous property losses [3-4].

Although Taiwan is well known for its achievements in inventing high-tech products, studies and research related to lightning rods are quite few and weak, and most of the present lightning rod devices are still imported from abroad. To improve the current situation, experiments were conducted on different lightning rods to find valuable research results that would benefit Taiwanese scientists in inventing Taiwan-based lightning rods. With the lightning rod adapted to the living environment of Taiwan, the heavy dependencies on imported lightning rod

*Corresponding author: Department of Electrical Engineering National Chin-Yi University of Technology Taichung-TAIWAN

devices, as well as the device maintenance fees, could then be reduced; a great step forward in the Taiwanese high-tech engineering field would also be achieved [5-7].

When the conventional lightning rod functions, the ground potential is raised and the extremely high voltage generated from it can cause harm to electric appliances. In addition, when installing the ground device, the electric resistance has to be set and maintained at certain values in accordance with the laws. In order to improve the disadvantages that a conventional lightning rod has, in this study, experiments were conducted to analyze the differences between the Franklin rod and 3 other modern lighting rods in the simulation system to investigate their effectiveness. With the findings, a remolded and well-performing lightning rod was then designed and recommended. Moreover, it could be expected that this research would benefit people’s living standards as well as domestic research in terms of improving and developing an advanced lightening rod [8-10].

2. Predischarge lightning rod discharge theory

Based on electromagnetic theory, it could be recognized that in order to satisfy the electrostatic field, the differentiation formula and integration formula could be applied to state the problems occurring from it and then solve them with relevant boundary conditions. Generally, the process of solving electromagnetic engineering problems is much more complicated; thus, numerical analysis would be the appropriate method for figuring out solutions. Among so many numerical analysis methods, the finite element method is the most effective and widely applied one [11-13].

Since lighting strokes occur as thunderclouds discharge down to the earth, it is then vital to calculate the electric field around the thunderclouds and the changes that happen. When the ground potential is lower than the air potential, in fine weather, the electric field on the ground would then be a positive one with a value around 100 V/m .

From the method of imaging [14], it is known that the earth’s surface (ground) is a conducting plane of infinite extent and depth. Therefore, if we are given a point charge Q at a distance H above the ground, we can obtain the imaginary charge -Q at the same distance away on the other side of the ground (as shown in Figure 1). This electric field can be described as follows:

$$E_{tot} = \frac{2QH}{4\pi\epsilon_0(H^2 + D^2)^{3/2}} \tag{1}$$

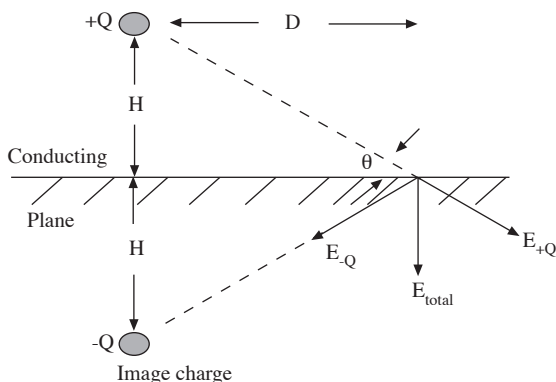


Figure 1. The strength of point charges in the sky to the strength of the ground electric field.

As can be seen above, D is the horizontal distance between the observation site and the charges. The electric field is a positive and vertically downward one, and the electric dipole moment is $M = 2 QH$. In the model of the electric dipole moment, when the upper part of a cloud contains a positive charge (Q_p) at height H_p and the bottom part has a negative charge (Q_N) at height H_N , then the electric field would be:

$$E = \frac{2}{4\pi\epsilon_0} \left[\frac{Q_p H_p}{(H_p^2 + D^2)^{3/2}} - \frac{Q_N H_N}{(H_N^2 + D^2)^{3/2}} \right]. \tag{2}$$

When the observation site is far from the thunderclouds, the electric field would be a positive one; however, when the site is close to the thunderclouds, the electric field would then appear to be negative. The negative lightning emitted from the clouds to the ground will decrease the negative charges inside a cloud by the amount of ΔQ_N and result in changes of the value of the ground electric field greater than zero.

$$\Delta E_{NG} = \frac{2}{4\pi\epsilon_0} \frac{\Delta Q_N H_N}{(H_N^2 + D^2)^{3/2}} \tag{3}$$

When the lightning stroke causes positive charges inside the thunderclouds, decreasing the value of ΔQ_p , the variation of the ground electric field would be less than zero.

$$\Delta E_{NG} = \frac{2}{4\pi\epsilon_0} \frac{\Delta Q_N H_N}{(H_N^2 + D^2)^{3/2}} \tag{4}$$

When lightning happens only within the thunderclouds, the decreasing quantity of the positive charge would be equal to that of the negative charges, and its electric field would be presented as follows:

$$\Delta E_{NP} = \frac{2\Delta Q}{4\pi\epsilon_0} \left[\frac{H_p}{(H_p^2 + D^2)^{3/2}} - \frac{H_N}{(H_N^2 + D^2)^{3/2}} \right]. \tag{5}$$

When the D value is small, then $\Delta E_{PN} > 0$; conversely, when the D value is large, then $\Delta E_{PN} < 0$. As the distance between the observation site and the thunderclouds is much greater than distance H_p , $\Delta E_{PN} < 0$. Based on these findings, it could be assumed that among all lightning that happens, 40% is generated from clouds and then emitted downward to the earth, and among that lightning, 90% is negative.

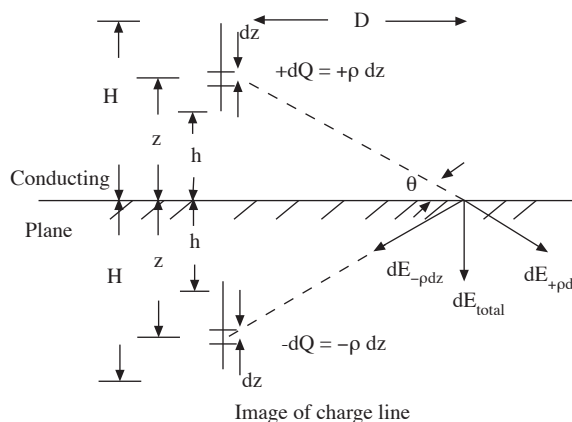


Figure 2. The strength of leader charges in the sky to the strength of the ground electric field.

To calculate the electric field in the leader process, it is suggested to assume that the leader is a vertical line filled with electricity. In the ideal condition, its electric charges are spread evenly or are in a cylindrical symmetry, as shown in Figure 2. Its electric field would be:

$$E_{tot} = \frac{2\rho}{4\pi\epsilon_0} \left[\frac{1}{(D^2 + h^2)^{3/2}} - \frac{1}{(D^2 + H^2)^{3/2}} \right] \tag{6}$$

Assuming that the length of the leader is p and the quantity of charges decreasing in the thunderclouds is Q , then the change of the electric field would be:

$$\Delta E_S = -\frac{2\rho\ell H}{4\pi\epsilon_0 (H^2 + D^2)^{3/2}} \tag{7}$$

Based on the above, it could be expected that the electric field of a downward leader would be:

$$\Delta E = \frac{2\rho}{4\pi\epsilon_0 D} \left[\frac{1}{(1 + \frac{h^2}{D^2})^{3/2}} - \frac{1}{(1 + \frac{H^2}{D^2})^{3/2}} - \frac{H-h}{D} \frac{1}{(1 + \frac{H^2}{D^2})^{3/2}} \right] \tag{8}$$

In terms of calculating the electric field around the lightning rod, only the ring charge would appear at a different Z-standard; point charges and charges (x_t, y_t, z_t) would stay at the top of the lightning rod, as shown in Figure 3. If N_z is present as part of the charges existing in the clouds and the lightning rod, then the total number of unknown charges inside the lightning rod would be $(N_z \times M) + 1$.

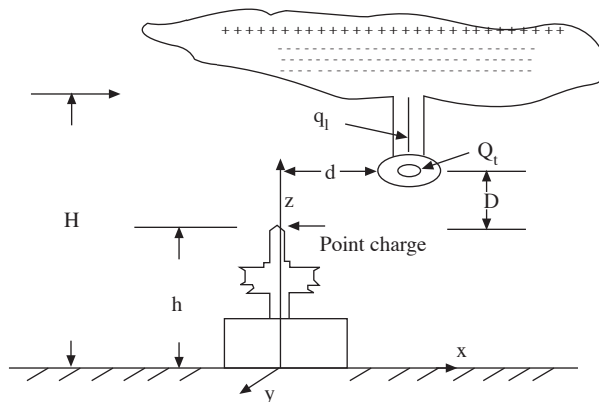


Figure 3. Simulated distributions of the downward negative charges and distribution of charges in the lightning rod.

3. Operation and components of a discharge lightning rod

The circuit system of a discharge lightning rod is composed of an autostarting and high-voltage emitting device, a power module, an operating system, an insulation system, and a vertical gliding dual instantaneous discharge device. The structure of a real discharge lightning rod is seen in Figure 4.

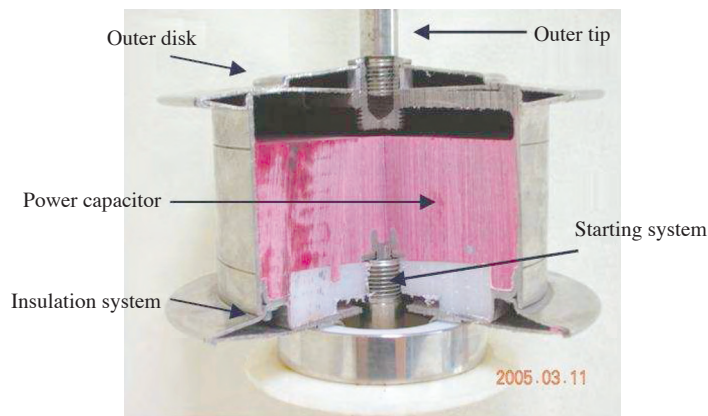


Figure 4. Components of a discharge lightning rod.

1) Auto starting and high-voltage pulse emitting device

This device comprises 3 systems (atmospheric electricity capacitor, starting system, and lightning flow grounding system), and their electrons are protected by the other 2 instantaneous discharge systems and insulation materials.

2) The energy module and the operating system are composed of the following devices.

1. High-voltage pulse discharge device: Energy from the potential gradient between the thunderclouds and the ground would pass through the inductance amplifier and be stored by the buffer register. This allows high-voltage pulses to ionize air instantaneously. As a result, the intensity of the electric field around the lightning rod would be increase, which would benefit increasing the altitude of the lightning discharge (performed by an erected conventional lightning rod).
2. Capacitance transmitter: The interval between the shell of the lightning rod and the grounding central axis forms a capacitor. Once the thunder leader is generated, this capacitor would be filled with charges containing the same voltage as the shell of the lightning rod and the grounding central axis, and it serves as a communication medium to prevent neutralization among the positive charges from the lightning rod and negative charges. This allows the negative charges to discharge adequately and not pass through the energy module. To be precise, if negative charges pass through the lightning rod and travel to the ground, they would do harm to the energy module. Once all charges are released, the operation of the medium would return to normal and the lightning rod would be ready for its next task.
3. Insulation system: The insulation system of a lightning rod could endure harm caused by bad weather such as heavy rains, snow, winds, or thunderclouds. Moreover, the second insulation layer could prevent the lightning rod from being corroded by acid or alkaline substances.

4. Simulating electric fields of different kinds of lightning rods

4.1. Analysis of patterns of different lightning rods

In this section, 4 types of lightning rods were input into a software-simulated 2D electric field to detect protective coverage and select the most effective lightning rod. Emission of positive charges from a lightning rod would happen only when the electric field surrounding it has a value greater than 50 kV/m; thus, in this 2D system,

the electric field of the lightning rods was set as 200 kV and the charges at the bottoms of the clouds were set as negative ones. In addition, the width of the building was set as 920 cm, with a height of 5000 cm and a distance between the top of the lightning rod and the ground of 5070 cm. As presented in Figures 5-8, it could then be understood how the different types of lightning rods performed in the simulated 2D electric field.

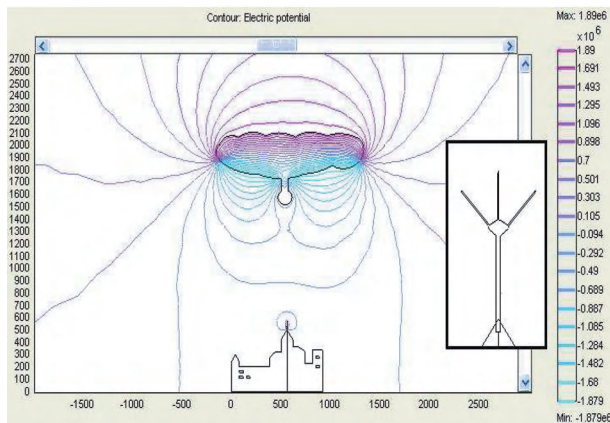


Figure 5. Lightning rod 1 in 2D simulation.

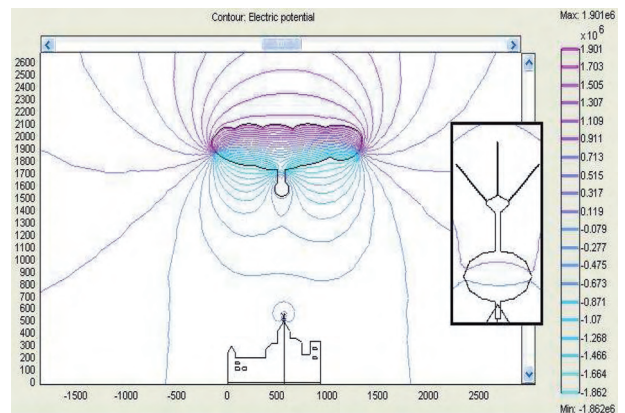


Figure 6. Lightning rod 2 in 2D simulation.

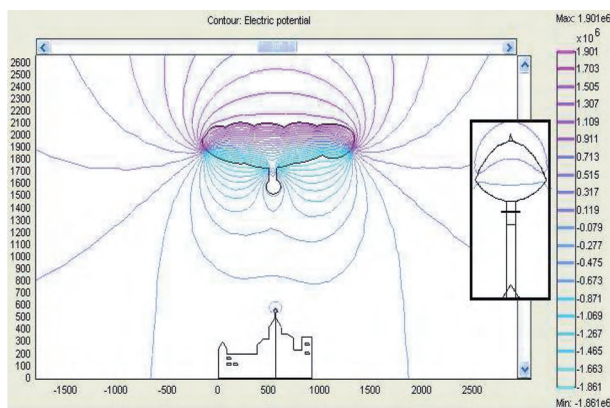


Figure 7. Lightning rod 3 in 2D simulation.

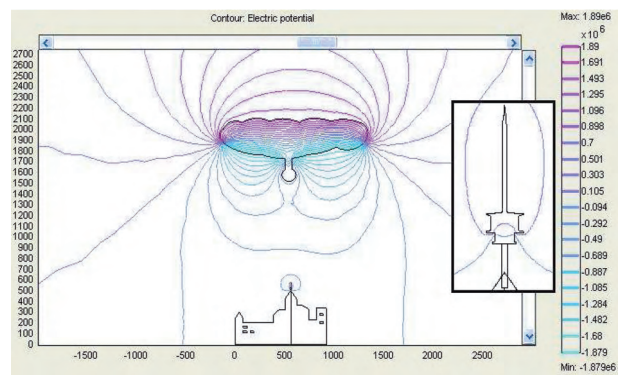


Figure 8. Lightning rod 4 in 2D simulation.

The static electric field was applied to analyze the neutralization altitude, the electric field inside the building, and the influenced areas of these 4 lightning rods. The neutralization altitude was measured from the top of the lightning rod up to the electric field, where it was zero. The higher the neutralization altitude is, the larger a protecting angle is. In terms of the electric field inside a building, the width of the building was identified as an abscissa, from 0 to 920. The influenced area of a lightning rod was also assumed to be an abscissa, from -1000 to 2000. The smaller the influenced area is, the less damage there is to the protected objects; Figure 9 reveals that lightning rod 3 created the smallest influenced area. In terms of the neutralization altitude, the higher the neutralization altitude is, the less lightning would damage the protected building; from Figure 9, it can be seen that lightning rod 1 performed best.

4.2. Different radii of the lightning rod disk

In this section, the radii of the disk of lightning rod 4 were designed in different lengths, 7, 8.45, 9, and 10 cm, to analyze their effects on the neutralization altitude and influenced area. As seen in Figure 10, when the

radius was 7 cm, the influenced area was the smallest; when the radius was 10 cm, the neutralization altitude then appeared to be the highest. The larger a disk radius is, the higher the achieved neutralization altitude, and vice versa.

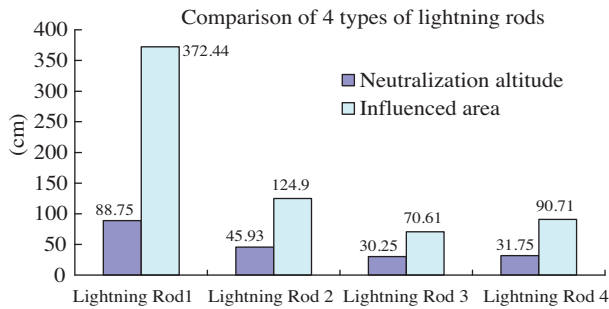


Figure 9. Lightning rods shown in 2D simulation.

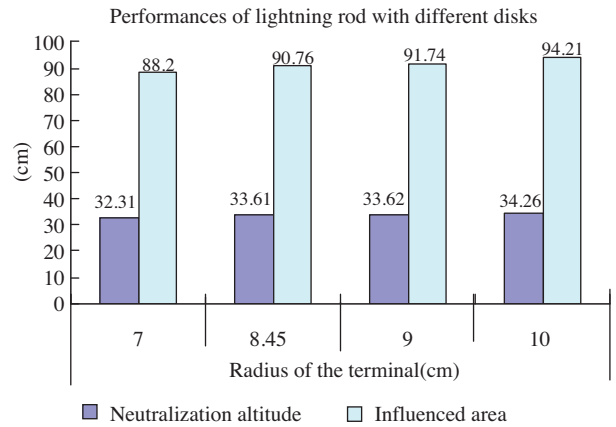


Figure 10. Simulated performances of lightning rod 4 with disks of different radii.

4.3. Different radii of lightning rod terminal

In this section, the radii of the terminal of lightning rod 4 were designed at different lengths, 0.875, 1, 2, and 3 cm, to analyze its effects on the neutralization altitude and influenced area. From Figure 11, it can be seen that when the radius was 0.875, the influenced area was the smallest; when the radius was 3 cm, the neutralization altitude was the highest. As a result, it could be concluded that the larger a terminal radius is, the higher the neutralization altitude is, and vice versa.

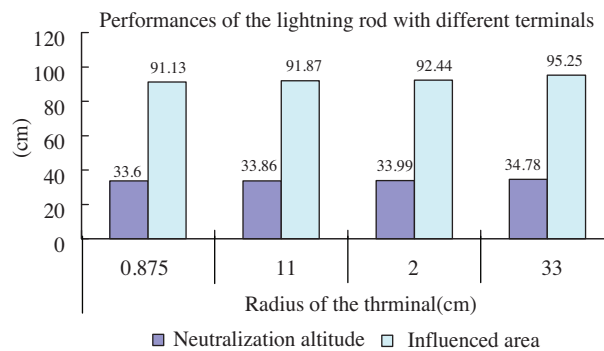


Figure 11. Performances of lightning rod 4 with terminals presented in different radii.

4.4. Synthetic analysis of different lightening rods

Based on the findings above, it was discovered that when the disk radius of a lightning rod is around 8-9 cm and the terminal radius is 1-2 cm, the best performance of a lightning rod can be expected. This finding was generalized from 2 prospects: the highest neutralization altitudes (when the disk radius is 8.5 cm and the terminal radius is 1.7 cm, as shown as Figure 12) and the smallest influence area (when the disk radius is 8 cm and the terminal radius is 1.8 cm, as displayed in Figure 13).

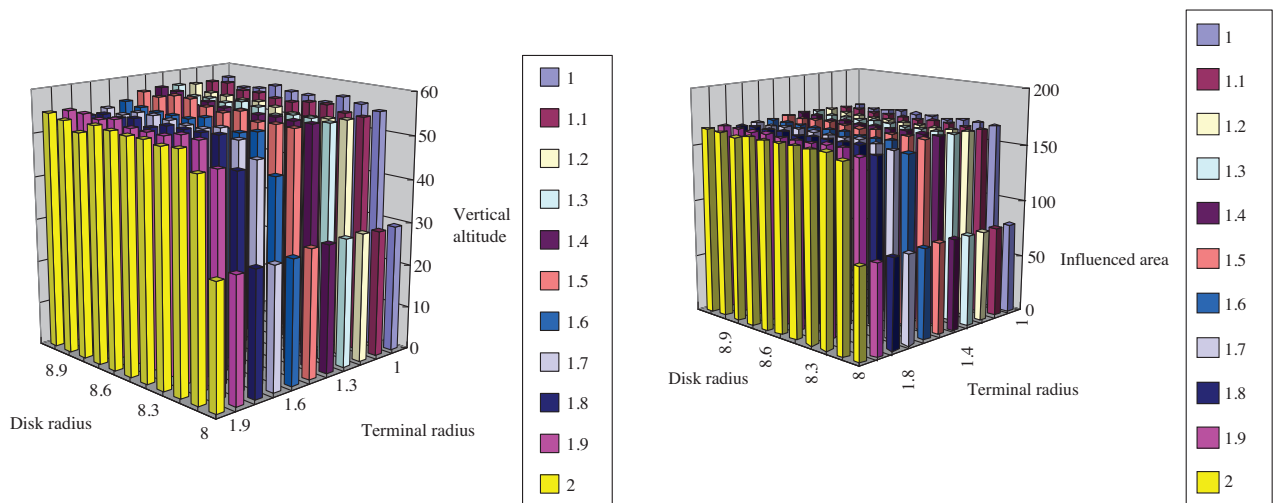


Figure 12. Synthetic comparisons of the neutralization altitudes achieved by different lightning rods.

Figure 13. Synthetic comparisons of the influenced areas achieved by different lightning rods.

Based on the data in Figure 14, it can then be seen that the lightning rod with a disk radius of 8.5 cm and a terminal radius of 1.7 cm was the best performing lightning rod.

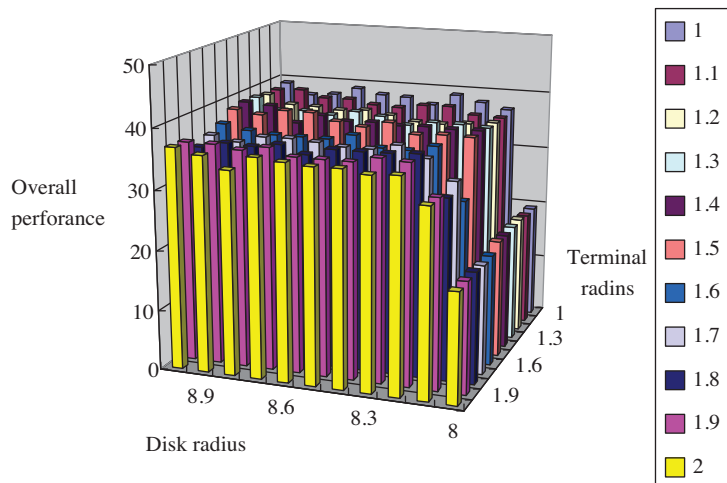


Figure 14. Synthetic comparison of efficiency of different lightning rods.

5. Conclusions

According to the analyzed results above, several conclusions were made and can be stated as follows.

1. Lightning rod 3 had the smallest influenced area and lightning rod 1 reached the highest neutralization altitude. The higher the neutralization altitude, the less damage to the protected buildings.
2. The optimal disk radius for lightning rod 4 was 7 cm, because its influenced area was the smallest one; however, as the disk radius of lightning rod 4 reached 10 cm, the highest neutralization altitude was achieved. In terms of the terminal radius, when the radius was 0.875 cm, the influenced area was the smallest one; however, when the radius was 3 cm, the highest neutralization altitude could be expected.

3. It is suggested that a lightning rod with a disk radius of 8.5 cm and a terminal radius of 1.7 cm would generate the best performance. Among the 4 studied types of lightning rods, lightning rod 1 required fewer materials and lower costs.

References

- [1] D. Dustegor, S.V. Poroseva, M.Y. Hussaini, S.L. Woodruff, "Structural analysis for assessment of monitoring possibilities: application to simple power system topologies," IEEE International Conference on Power and Energy Society General Meeting, pp. 1-7, 2008.
- [2] K.G. Ravikumar, N.N. Schulz, A.K. Srivastava, "Distributed simulation of power systems using real-time digital simulator," IEEE International Conference on Power Systems Conference and Exposition, pp. 1-6, 2009.
- [3] T. Miyazaki, S. Okabe, S. Sekioka, "An experimental validation of lightning performance in distribution lines," IEEE Trans. Power Del., Vol. 23, pp. 2182-2190, 2008.
- [4] S. Sekioka, M.I. Lorentzou, M.P. Philippakou, J.M. Prousalidis, "Current-dependent grounding resistance model based on energy balance of soil ionization", IEEE Trans. Power Del., Vol. 21, pp. 194-201, 2006.
- [5] M. Lei, J. Zeng, G. Liu, "Simulation analysis of flashover characteristics of 220kV composite insulators based on finite-element method," IEEE International Conference on Properties and Applications of Dielectric Materials, pp. 697-700, 2009.
- [6] O.D. Thiele, V. Beachum, "Case studies in arc flash reduction to improve safety and productivity," IEEE International Pulp and Paper Industry Technical Conf., pp. 93-99, 2008.
- [7] M.H. Shwehdi, "Lightning thunderstorms day maps for Saudi Arabia," IEEE International Conference on Power System Technology and IEEE Power India Conference, pp. 1-6, 2008.
- [8] V. Javor, P.D Rancic, "Electromagnetic field in the vicinity of lightning protection rods at a lossy ground," IEEE Trans. Electromagnetic Compatibility, Vol. 51, pp. 320-330, 2009.
- [9] L. Hua, P. Tingting, Z. Yinxue, S. Jing, L. Zhiqiang, "Electromagnetic tomography based on finite element method and improved genetic algorithm", IEEE International Conference on Industrial Mechatronics and Automation, pp. 430-433, 2009.
- [10] M. Boutaayamou, R.V. Sabariego, P. Dular, "Electrostatic analysis of moving conductors using a perturbation finite element method", IEEE Trans. Magnetics, Vol. 45, pp. 1004-1007, 2009.
- [11] A. Andreotti, D. Assante, F. Mottola, L. Verolino, "Fast and accurate evaluation of the underground lightning electromagnetic field", IEEE International Conference on Electromagnetic Compatibility, pp. 1-6, 2008.
- [12] F. D'Alessandro, C.J. Kossmann, A.S. Gaivoronsky, A.G. Ovsyannikov, "Experimental study of lightning rods using long sparks in air", IEEE Trans. Dielectrics and Electrical Insulation, Vol. 11, pp. 638-648, 2004.
- [13] L. Jiang, F. Kong, "Finite element method and emulator based on grid technology", IEEE International Conference on Control, pp. 182-186, 2008.
- [14] B.S. Guru, G.R. Hiziroğlu, *Electromagnetic Field Theory Fundamentals*, PWS Publishing Company, 1998.